JACS
JOURNAL OF THE AMERICAN CHEMICAL SOCIETY
Article
pubs.acs.org/JACS

Harnessing Yeast Peroxisomes for Biosynthesis of Fatty-Acid-Derived Biofuels and Chemicals with Relieved Side-Pathway Competition

Yongjin J. Zhou,*[,†,‡,#] Nicolaas A. Buijs,[†,⊥,#] Zhiwei Zhu,[†,‡] Diego Orol Gómez,[†] Akarin Boonsombuti,[†] Verena Siewers,[†,‡] and Jens Nielsen*[,†,‡,§,∥]

[†]Department of Biology and Biological Engineering, [‡]Novo Nordisk Foundation Center for Biosustainability, Chalmers University of Technology, SE-41296 Gothenburg, Sweden

[§]Novo Nordisk Foundation Center for Biosustainability, Technical University of Denmark, DK-2800 Kgs, Lyngby, Denmark

[∥]Science for Life Laboratory, Royal Institute of Technology, SE-17121 Stockholm, Sweden

Supporting Information

ABSTRACT: Establishing efficient synthetic pathways for microbial production of biochemicals is often hampered by competing pathways and/or insufficient precursor supply. Compartmentalization in cellular organelles can isolate synthetic pathways from competing pathways, and provide a compact and suitable environment for biosynthesis. Peroxisomes are cellular organelles where fatty acids are degraded, a process that is inhibited under typical fermentation conditions making them an interesting workhouse for production of fatty-acid-derived molecules. Here, we show that targeting synthetic pathways to peroxisomes can increase the production of fatty-acid-derived fatty alcohols, alkanes and olefins up to 700%. In addition, we demonstrate that biosynthesis of these chemicals in the peroxisomes results in significantly decreased accumulation of byproducts formed by competing enzymes. We further demonstrate that production can be enhanced up to 3-fold by increasing the peroxisome population. The strategies described here could be used for production of other chemicals, especially acyl-CoA-derived molecules.

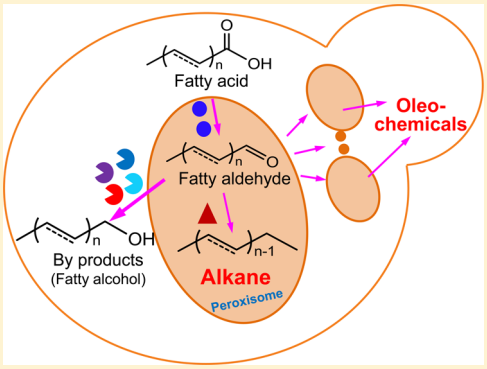

INTRODUCTION

Efficiency and selectivity are key factors for development of chem-[1] and biocatalysts,[2] as they determine the overall process economy. However, for whole-cell biocatalysts, construction of synthetic pathways for biochemical production is often hampered by competing pathways and/or insufficient precursor supply. For example, while constructing a synthetic yeast cell factory for production of alkanes, ideal drop-in biofuels, we found that there was a much higher accumulation of byproduct fatty alcohols than alkanes.[3,4] The high level accumulation of fatty alcohols may be attributed to promiscuous aldehyde reductases/alcohol dehydrogenases (ALR/ADHs) in the cytosol that compete for the fatty aldehyde intermediates[5] with the less efficient fatty aldehyde deformylating oxygenase (ADO, k_{cat} < 0.1 min^{-1}).[6] Thus, novel approaches are urgently required to increase the productivity of alkanes and other oleo-chemicals and biofuels in yeast.[7]

Compartmentalization of the biosynthetic pathways could avoid the strong competition for metabolic precursors and intermediates from competing pathways, which would decrease the accumulation of byproducts. Though mitochondria have been engineered for production of a group of chemicals such as isoprenoids[8,9] and fusel alcohols,[10] the mitochondrial ADHs[11] make it not suitable for alkane production since ADHs will compete for the fatty aldehyde. In contrast, there is no reported fatty aldehyde-preferring ALR/ADHs localized in the peroxisome.[12] Thus, targeting the synthetic pathway into the peroxisomes may prevent the loss of the fatty aldehyde intermediates toward fatty alcohol biosynthesis by secluding the alkane biosynthetic pathways from the cytosolic competing ALR/ADHs. Furthermore, it has been suggested that the peroxisomes have many potential advantages for the production of fatty acyl-CoA-derived chemicals, such as a more compact space for improved substrate channelling.[13] Furthermore, there is a peroxisomal NADP-dependent isocitrate dehydrogenase isoenzyme Idp3 that is providing NADPH,[14−17] which is required for the reduction of acyl-CoAs or fatty acids toward highly reduced molecules such as alkanes and alcohols.

For these reasons, we decided to evaluate whether the yeast peroxisomes can be harnessed to produce fatty-acid-derived chemicals and biofuels: fatty alcohols, alkanes and olefins. To demonstrate this concept, we first targeted a one-step pathway for production of fatty acyl-CoA-derived fatty alcohols. We then constructed a multistep pathway for fatty-acid-derived alkane biosynthesis, which in the cytosol suffers from strong competition from fatty alcohol production catalyzed by efficient endogenous ALR/ADHs. By using this model system, we

Received: July 22, 2016
Published: October 18, 2016

DOI: 10.1021/jacs.6b07394
J. Am. Chem. Soc. 2016, 138, 15368−15377

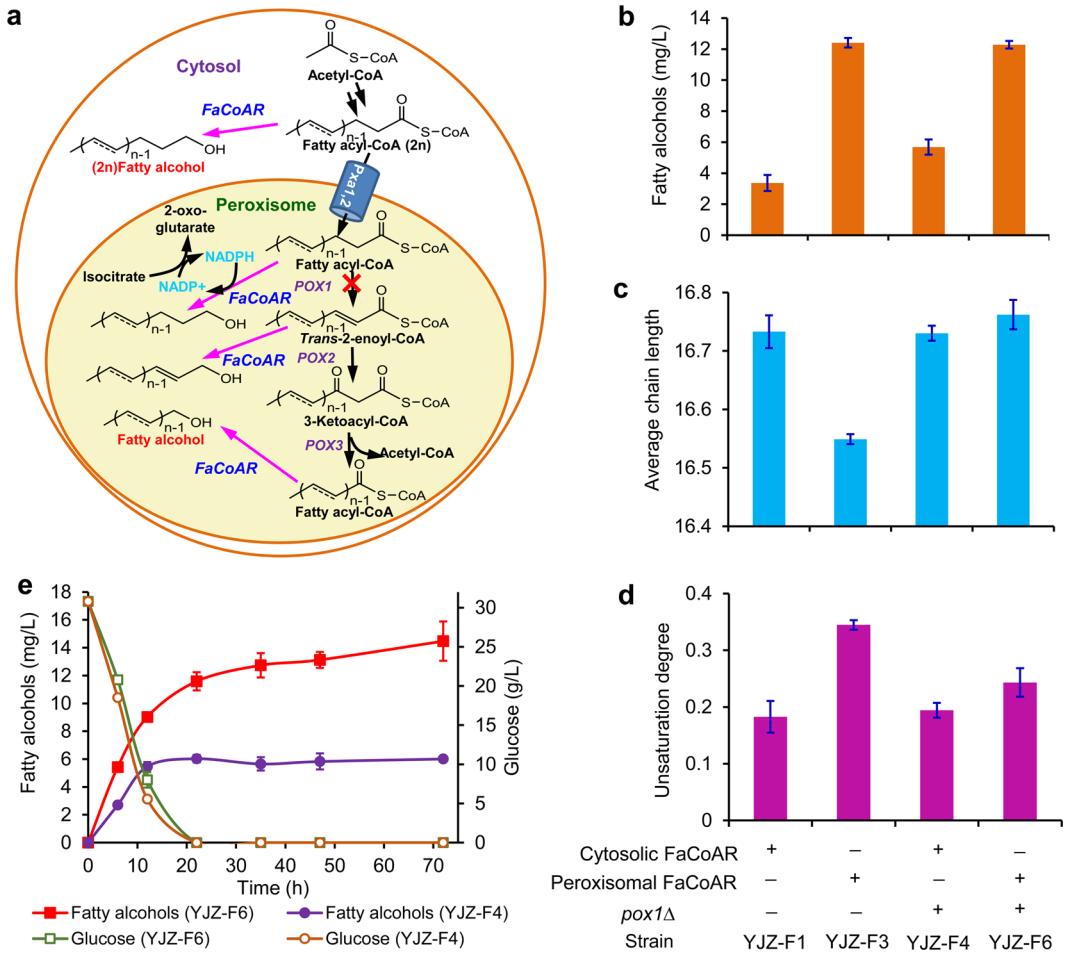

Figure 1. Peroxisomal compartmentalization improved production of fatty acyl-CoA derived fatty alcohol. (a) Schematic view of metabolic pathway for fatty alcohol production. (b–d) Titers, average chain lengths, and unsaturation degrees of fatty alcohols. YJZ-F1 and YJZ-F3 are strains that express cytosolic or peroxisomal FaCoAR, respectively, in wild-type background; YJZ-F4 and YJZ-F6 represent cytosolic or peroxisomal expression of FaCoAR, respectively, in a *pox1*Δ background. Unsaturation degrees represent the average double bond number in the fatty alcohols. (e) Time profile of fatty alcohol production and glucose concentration. All data represent the mean ± SD of three yeast clones.

clearly show that peroxisome compartmentalization not only increases the production of target molecules, but also decreases byproduct formation. We further show that enhancing the peroxisome population by engineering the peroxisomal biogenesis can improve the biosynthesis. Finally, we show that the advantage of peroxisomal pathway localization for improving production of fatty-acid-derived chemicals is generalizable as it also enables increased olefin production. Thus, our results demonstrate that peroxisome targeting is a feasible strategy for improving production of fatty-acid-derived chemicals and we anticipate that future research could extend this to be used for production of other acyl-CoA-derived chemicals.

RESULTS

A Proof of Concept: Peroxisomal Production of Fatty Acyl-CoA-Derived Fatty Alcohols. First, we needed to verify that the peroxisomes contain a sufficient level of precursors and cofactors (e.g., NADPH) to support the biosynthesis of fatty-acid-derived molecules. For this we constructed a one-step fatty alcohol synthetic pathway (Figure 1a) by expressing a bifunctional fatty acyl-CoA reductase (FaCoAR) from *Marinobacter aquaeolei*.[18] We first compared different contexts of the peroxisomal targeting signal, and found that when the signal per2 (GGGSAAVKLSQAKSKL) was used for targeting FaCoAR to the peroxisome we obtained the highest fatty alcohol production (Figure S1). Fluorescence microscopy analysis verified that per2 tagged FacoAR efficiently targeted to the peroxisomes (Figure S2). Peroxisomal targeting of FaCoAR increased fatty alcohol production by 2.7-fold to 12.4 mg/L in a wild-type background (strain YJZ-F1 vs YJZ-F3, Figure 1b). Blocking fatty acid degradation, by deleting the fatty acid oxidase encoding gene *POX1* involved in β-oxidation, increased cytosolic fatty alcohol production by 68%, but blocking β-oxidation did not increase production of peroxisomal fatty alcohols (Figure 1b), which indicated that peroxisomal FaCoAR could efficiently compete for fatty acyl-CoA with the β-oxidation pathway. It is worth mentioning that peroxisomal targeting of FaCoAR resulted in a slightly higher proportion of shorter (Figure 1c) and unsaturated (Figure 1d) fatty alcohols than the cytosolic pathway in a wild-type background (strain YJZ-F1 vs YJZ-F3). The product profiles were similar in a *pox1*Δ background with peroxisomal and cytosolic FaCoAR (train YJZ-F4 vs YJZ-F6, Figure 1c,d), which suggested that an intact β-oxidation pathway provided more shorter and unsaturated fatty acyl-CoA intermediates as substrates for peroxisomal fatty alcohol biosynthesis.

The strain YJZ-F4 carrying the cytosolic FaCoAR reached the highest fatty alcohol titer after 12 h of growth on glucose,

DOI: 10.1021/jacs.6b07394
J. Am. Chem. Soc. 2016, 138, 15368–15377

while the peroxisome pathway containing strain YJZ-F6 had a higher fatty alcohol production rate in the glucose phase and kept producing fatty alcohols after all glucose had been consumed (Figure 1e). These results demonstrated that peroxisomal compartmentalization improved fatty alcohol production with an elevated productivity and a prolonged biosynthesis span.

To verify the applicability of this strategy in other genetic background, we targeted FaCoAR to the peroxisomes in a fatty acyl-CoA overproducing strain JV03[19] with blocked fatty acyl-CoA consuming pathways (including β-oxidation, sterylester and triacylglycerol biosynthesis) (Figure 2a). We observed that

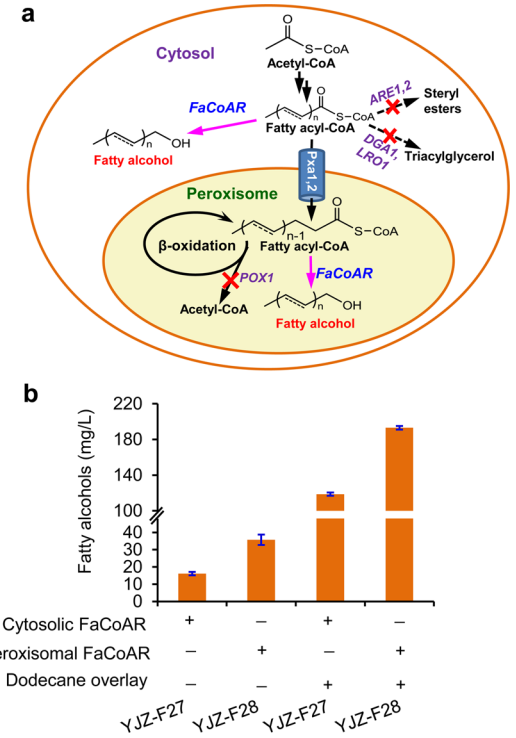

Figure 2. Peroxisomal compartmentalization improved fatty alcohol production in a fatty acyl-CoA overproducing strain. (a) Schematic view of the metabolic pathways for fatty alcohol production with blocked fatty acyl-CoA consuming pathway. (b) Fatty alcohol titers. The data represent the mean ± SD of three yeast clones.

peroxisomal compartmentalization improved fatty alcohol production by 220% (strain YJZ-F27 vs YJZ-F28, Figure 2b). Using a dodecane overlay for in situ extraction, strain YJZ-F28 carrying peroxisomal FaCoAR also had a 63% higher fatty alcohol production (193 mg/L) compared to the cytosolic pathway strain YJZ-F27 (Figure 2b), which is comparable with a previous study with shake flask cultivation.[20] These results show that a higher fatty acyl-CoA supply is helpful for fatty alcohol production catalyzed by FaCoAR and suggest that peroxisomes might have a higher level of precursor for biosynthesis of fatty-acid-derived chemicals. This gave us confidence to engineer the peroxisomes for producing other fatty-acid-derived oleo-chemicals and biofuels.

Peroxisomal Production of Fatty-Acid-Derived Alkanes. Next, we engineered the peroxisomes for production of alkanes, an ideal gasoline and diesel substitute because of their high similarity to fossil oil-derived liquid fuels.[21] We recently established long-chain alkane production in *Saccharomyces cerevisiae* by introducing fatty acyl-CoA[3] or free fatty acid (FFA)[4] based pathways. However, the titers were extremely low (<1 mg/L) and there were much higher accumulation of fatty alcohols.[3,4] A limited availability of fatty aldehydes was also observed in a recent study on alkane biosynthesis in yeast.[22] The main reasons might be that aldehyde-deformylating oxygenase (ADO) has a low efficiency (k_{cat} < 0.1 min^{-1}) and is also inhibited by its own byproduct hydrogen peroxide (H_2O_2).[6] Furthermore, there are a large number of endogenous promiscuous ALR/ADHs that compete for the intermediate fatty aldehyde[23] in *S. cerevisiae*.[24] Peroxisomes have at least three potential advantages for alkane production (Figure 3a): they (1) provide spatial proximity for substrate channelling;[25] (2) contain the peroxisomal catalase Cta1 that may relieve the H_2O_2 inhibition of the ADO; (3) seclude competing enzymes such as aldehyde reductases, which would decrease fatty alcohol accumulation. We thus compartmentalized the *Synechococcus elongatus* fatty acyl-CoA derived pathway (SeAAR, SeADO with the electron transfer system of *E. coli*, ferredoxin EcFd and ferredoxin reductase EcFNR) into the peroxisomes (Figure S2), which enabled a 40% increase of alkane production in a wild-type background (Figure 3b). We also evaluated an alternative ADO from *Nostoc punctiforme* PCC73102[26] (NpADO), but this was found to be less efficient than SeADO for alkane production in the peroxisomes (Figure S3). We further evaluated the cognate electron transfer system (SeFNR and SeFd)[27] from *S. elongates* and found that this improved alkane production slightly compared with the *Escherichia coli* system and was thus used further on. However, an engineered self-sufficient aldehyde deformylating oxygenases fused to the electron transfer system, which had improved activity in vitro,[28] resulted in a lower alkane titer compared with the native enzymes (Figure S3).

Our previous study showed that a FFA based pathway was more efficient than a fatty acyl-CoA derived pathway in regards of cytosolic alkane production in yeast.[4] We therefore targeted an FFA based pathway to the peroxisome by expressing a *Mycobacterium marinum* carboxylic acid reductase (MmCAR)[29] and its activation cofactor-4′-phosphopantetheinyl transferase NpgA from *Aspergillus nidulans* (Figure 3a). Similarly, peroxisomal compartmentalization of the FFA based pathway (strain A10) resulted in a 90% higher alkane titer compared with the cytosolic pathway, and a 200% higher alkane production (0.06 mg/L) compared with the peroxisomal fatty acyl-CoA-derived pathway in a wild-type background (Figure 3b).

We then tried to increase the fatty acid supply by deleting *POX1* to block β-oxidation. However, *POX1* deletion only led to a marginal improvement of alkane production (Figure 3c). Interestingly, deletion of *HFD1* encoding fatty aldehyde dehydrogenase increased alkane production by 10-fold, which was similar to the effect of *hfd1*Δ on cytosolic alkane biosynthesis (Figure 3c). It should be mentioned that *HFD1* deletion resulted in a 65-fold higher fatty alcohol accumulation with the cytosolic alkane biosynthesis pathway, indicating Hfd1 had a much higher efficiency than ALR/ADHs in competing for fatty aldehydes ($v_{Hfd1} > v_{ALR/ADHs}$). The much higher accumulation of fatty alcohols (11.18 mg/L) compared to alkanes (0.52 mg/L) showed the strong competition of ALR/ADHs over ADO ($v_{ALR/ADHs} > v_{ADO}$). Furthermore, MmCAR expressing strain A12 had a much higher fatty alcohol production (11.18 mg/L) compared to the background strain YJZ03 (1.52 mg/L) in an *hfd1*Δ strain, which suggested the

DOI: 10.1021/jacs.6b07394
J. Am. Chem. Soc. 2016, 138, 15368−15377

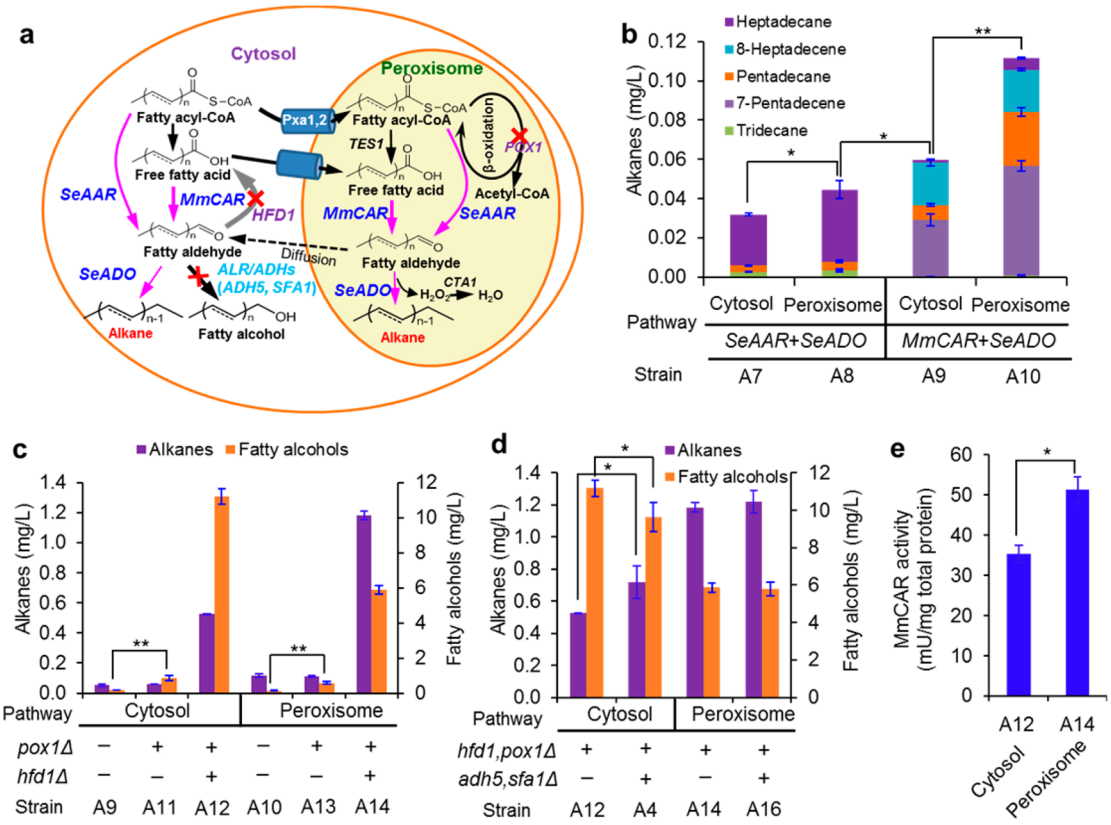

Figure 3. Peroxisomal compartmentalization improved alkane production. (a) Schematic view of the metabolic pathways for alkane production. (b) Peroxisomal compartmentalization improved the alkane production for both fatty acyl-CoA and fatty acid based pathways in a wild-type background. (c) Effect of peroxisome targeting on alkane production and fatty alcohol accumulation with the FFA based pathway. (d) Effect of deletion of alcohol dehydrogenase gene *ADH5* and aldehyde reductase gene *SFA1* on alkane production and fatty alcohol accumulation. (e) MmCAR activities in strains harboring the cytosolic (strain A12) and peroxisomal (strain A14) pathways. All data represent the mean ± s.d. (*P < 0.05; **P < 0.01, by Student's t test) of three yeast clones.

that heterologous alkane pathway provided much more fatty aldehydes compared to those generated by endogenous sphingolipid degradation.[3]

Peroxisomal compartmentalization resulted in significant and similar improvements (about 1-fold) for alkane production in different strain backgrounds. While the byproduct fatty alcohol titer decreased much more in the *hfd1*Δ background (50% decrease, strain A14 vs A12) than in the control background (32% decrease, strain A13 vs A11) (Figure 3c), fatty alcohol production was still much (5-fold) higher than alkane production in the *hfd1*Δ background. These results suggested that the fatty aldehydes may be able to diffuse across the peroxisomal membrane and then be converted to FFAs by Hfd1 in the cytosol, since the peroxisome membrane is permeable for metabolites smaller than 400 Da.[13]

Deletion of the cytosolic ALR/ADH genes *ADH5* and *SFA1* slightly increased cytosolic alkane production with decreased fatty alcohol accumulation, while their deletion had no effect on peroxisomal alkane production and fatty alcohol accumulation (Figure 3d). These observations suggested that the fatty aldehyde diffusion rate (v_{Diff}) was slower than the catalytic rate of ALR/ADHs but faster than the catalytic rate of ADO ($v_{ALR/ADHs} > v_{Diff} > v_{ADO}$), and thus the peroxisomal membrane could seclude ADO from the competing cytosolic ALR/ADHs. In summary, we speculate that the efficiency of fatty aldehyde consuming processes followed the order of $v_{Hfd1} > v_{ALR/ADHs} > v_{Diff} > v_{ADO}$ (reflected by the line width in Figure 3a).

We also evaluated enzyme activities and strain A14 carrying a peroxisomal pathway had a 45% higher MmCAR activity compared with strain A12 carrying the cytosolic pathway (Figure 3e), which probably owing to a more appropriate environment for protein function compared with the cytoplasm. Interestingly, the strain A14 with higher MmCAR activity had a much lower fatty alcohol accumulation. This was again in agreement with the observation that peroxisomal compartmentalization significantly increased alkane production by secluding the alkane biosynthetic pathways from the competing cytosolic ALR/ADHs, though Hfd1 seems to have a high affinity for the fatty aldehydes and therefore is able to convert fatty aldehydes that partly diffuse out of the peroxisomes. It should be mentioned that the increase of enzymatic activity (45% increase) is less than the alkane production improvement (100% increase) of peroxisomal pathway compared to cytosolic pathway. These results suggested that the higher alkane titer with the peroxisomal pathway was a combinatorial effect of improved enzymatic activity and relieved side-pathway competition by peroxisomal compartmentalization.

Engineering Peroxisomal Biogenesis for Improving Biosynthesis. Even though peroxisomal targeting significantly improved the production of alkanes, the titer needs to be further enhanced. As there are only a very small number of peroxisomes in cells grown on glucose (Figure 4d and Figure S2), we explored the opportunity to increase the peroxisome population in order to improve alkane production (Figure 4a).

DOI: 10.1021/jacs.6b07394
J. Am. Chem. Soc. 2016, 138, 15368−15377

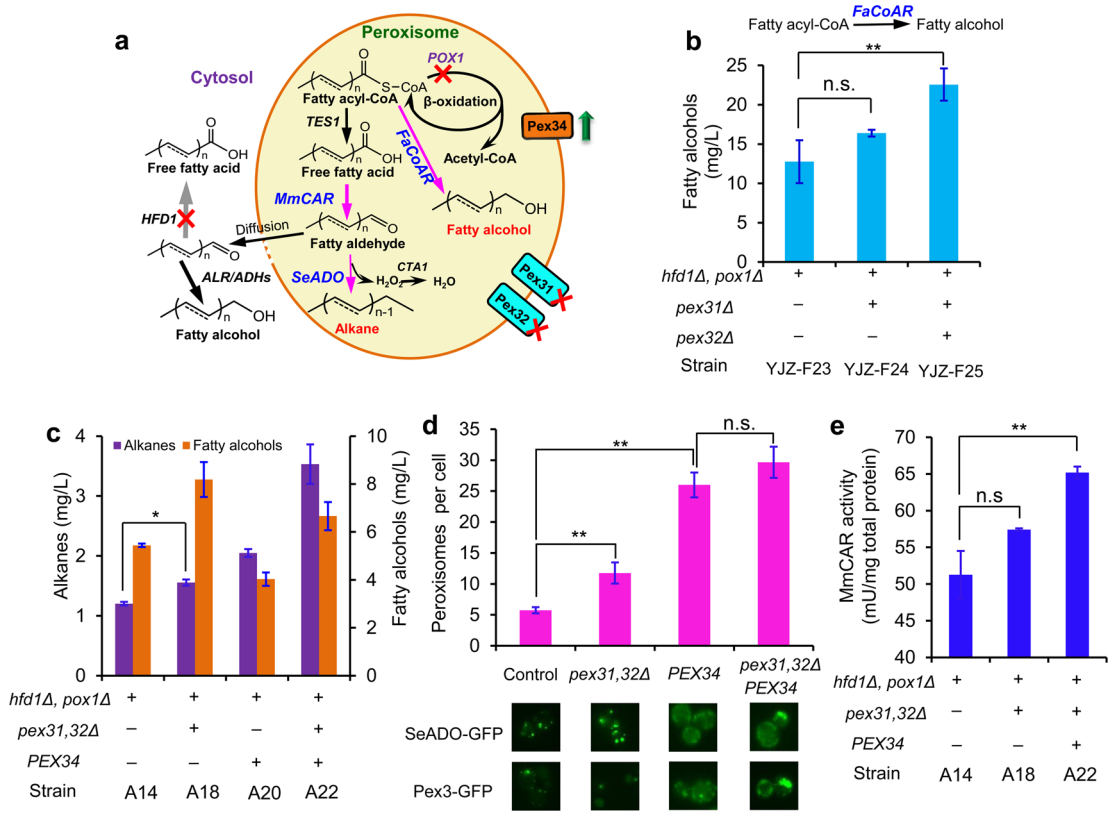

Figure 4. Engineering peroxisome population for improving biosynthesis. (a) Schematic view of the peroxisomal pathways for production of fatty acyl-CoA-derived fatty alcohols and FFA-derived alkanes. (b) Deletion of *PEX31* and *PEX32* improved production of fatty acyl-CoA-derived fatty alcohols. (c) Engineering peroxins for improving alkane production from free fatty acids. (d) Engineering of peroxins resulted in higher number of peroxisomes. The top panel shows the peroxisome number per cell and the bottom shows the fluorescence microscopy pictures of cells carrying the GFP-tagged matrix protein SeADO-GFP or membrane protein Pex3-GFP. (e) MmCAR activity in the corresponding strains at 48 h cultivation. All data represent the mean ± SD of three yeast clones, $^{*}P < 0.05$; $^{**}P < 0.01$; n.s., $p > 0.05$, by Student's t test.

Peroxisome biogenesis is highly controlled and the growth and division of peroxisomes are regulated by different mechanisms involving peroxins.[30] Several reports showed that different peroxisomal integral membrane proteins are involved in regulating peroxisome population. For example, Pex30-32 have been shown to be involved in peroxisome proliferation and their deletion resulted in increased peroxisome number and size.[31] As a proof of concept, we investigated the effect of combinatorial deletions of *PEX30-32* on the production of fatty acyl-CoA-derived fatty alcohols by using the available knockout strains in a S288C background.[31] Among the deletion combinations, *pex31,32*Δ increased fatty alcohol production by 20% for the peroxisomal pathway, but had a slightly negative effect on cytosolic pathway-based fatty alcohol production (Figure S4). A previous study showed that *pex31,32*Δ increased the peroxisome number and size,[31] which might contribute to the improvement of peroxisomal fatty alcohol production. We further introduced the *pex31,32*Δ double deletion into the CEN.PK derived strain YJZ03. With peroxisomal FaCoAR expression, *pex31*Δ increased fatty alcohol production by 28% and *pex31,32*Δ resulted in a more significant increase of fatty alcohol production (77%, Figure 4b). Fluorescence microscopy analysis of the cells showed that the *pex31,32*Δ strain contained more and larger peroxisomes (Figure 4d). Previous studies described that the peroxisome number in a *pex31,32*Δ strain increased as a result of oleic acid supplementation.[31] Here, we show that the double deletion also increased the peroxisome size and number in glucose-containing media.

We then implemented this strategy for improving alkane production. Consistently, the *pex31*Δ strain led to an increased alkane production by 22% and the *pex31,32*Δ strain exhibited a 25% higher alkane production (Figures S5 and 4c). However, the accumulation of byproduct fatty alcohols increased even more (by 50%), which might be attributed to a higher permeability of the peroxisome membrane for fatty aldehydes (which are then converted by cytosolic ALR/ADHs toward fatty alcohol biosynthesis). Actually, fluorescence microscopy showed that the peroxisomal membrane protein Pex3-GFP did not target to the peroxisome membrane properly, while matrix protein SeADO-GFP was properly localized to the peroxisomes (Figure 4d). These results suggest that deletion of *PEX31,32* results in changes in peroxisomal membrane structure or composition, which may in return also have resulted in changes in permeability.

Besides biogenesis induction by peroxins, some peroxisome integral membrane proteins are responsible for constitutive peroxisome division and may therefore serve as further engineering targets. Pex34 is such a peroxin that works together with Pex11 to control the peroxisome population of cells under conditions of both peroxisome proliferation and constitutive peroxisome division.[32,33] Overexpression of *PEX11* increased alkane production slightly (Figure S5c), which might be attributed to its pore forming activity that may perturb the peroxisome homeostasis.[34] *PEX34* overexpression significantly improved alkane production by 54% (Figure 4c), though the strain had a lower biomass yield (Figure S5b). More

DOI: 10.1021/jacs.6b07394
J. Am. Chem. Soc. 2016, 138, 15368−15377

importantly, the fatty alcohol accumulation in a *PEX34* overexpression strain A20 was 26% lower compared to the control strain (Figure 4c), which indicated that there was less diffusion of fatty aldehydes out of the peroxisomes in the *PEX34* overexpression strain and it did not have the same potential influence on the membrane structure as the *pex31,32*Δ strain. Consistently, fluorescence microscopy showed that *PEX34* overexpressing cells had more peroxisomes compared with the control strain, and both matrix protein SeADO-GFP and membrane protein Pex3-GFP targeted to the peroxisomes properly (Figure 4d). Combining PEX34 overexpression with the *pex31,32*Δ (strain A22) further increased alkane formation to 3.55 mg/L, which was 3-fold higher compared to the control (strain A14) and 7-fold higher compared to the titer obtained using a cytosolic pathway. It should be emphasized that the biomass specific alkane titer in strain A22 compared with strain A14 increased even more (3.5-fold) (Figure S6), because engineering of the peroxins slightly reduced the biomass yields in the shake flask cultures. These data show that the titers are positively correlated with the peroxisome number (Figure 4c and 4d), which could be regulated by engineering peroxisome biogenesis. Consistently, the increased number of peroxisomes resulted in higher MmCAR activity, which might contribute to the elevated alkane production (Figure 4e). It is worth mentioning that *PEX31,32* deletion and *PEX34* overexpression had no effect on cytosolic alkane production (Figure S7), which verified that engineering these peroxins actually increased the peroxisome number without interruption of cytosolic fatty acid metabolism.

Expanding Peroxisomal Compartmentalization for Olefin Production. We finally evaluated the use of peroxisomal compartmentalization for production of olefins, which are used as surfactants and lubricants. Olefins can be synthesized from free fatty acids by polyketide synthases,[35,36] H_2O_2-dependent P450 enzymes[37] and iron dependent fatty acid decarboxylases.[38] Cytosolic expression of a codon-optimized *oleT*, encoding a P450 fatty acid decarboxylase from *Jeotgalicoccus* sp. ATCC8456,[37] enabled production of olefins at 0.12 mg/L in a fatty acid overproducing strain YJZ06 (Figure 5). The main product was 1-heptadecene (C17:1), similar to a previous report.[39] This titer is higher than what was observed for expression in a *faa1,4*Δ strain by Chen et al.,[39] which could be due to differences in strain background and cultivation conditions. Since OleT is hydrogen peroxide-dependent, which could limit the reaction, a previous study by Liu et al.[40] sought to find alternative redox partners for this enzyme. Liu et al. fused OleT to a P450 reductase domain RhFRED from *Rhodococcus* sp. to render the enzyme NADPH-dependent. Furthermore, their study showed that *E. coli* flavodoxin and flavodoxin reductase can support OleT activity in vitro, but overexpression in vivo was not reported. Therefore, we tested both strategies. The OleT-RhFRED fusion protein decreased olefin production (Figure S8), similar to what was observed in the fatty acid overproducing *E. coli* strain by Liu et al. OleT together with the potential electron transfer system from *E. coli* (consisting of flavodoxin FldA and flavodoxin reductase EcFNR; FldA/FNR) increased olefin production by 20% (Figure 5b). Furthermore, overexpression of the molecular chaperones GroEL/GroES for improving P450 folding did not further increase olefin production (Figure S8). Alternatively, we expressed OleT together with FldA/FNR in the peroxisomes. Peroxisomal compartmentalization improved olefin production by 40% compared with the use of the cytosolic pathway (Figure 5b). These results demonstrated that peroxisomal compartmentalization can be used as a general strategy for producing oleo-chemicals that are derived from fatty acyl-CoAs or free fatty acids.

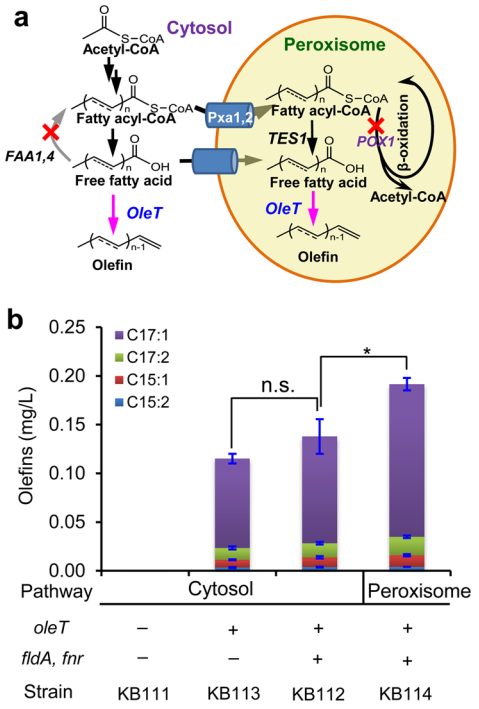

Figure 5. Peroxisomal compartmentalization improved olefin production in yeast. (a) Schematic view of the metabolic pathway. (b) Olefin titers from the corresponding strains. C15:2, 1,7-pentadecadiene; C15:1, 1-pentadecene; C17:2, 1,8-heptadecadiene; C17:1, 1-heptadecene. All data represent the mean ± SD of three clones. *$P < 0.05$; n.s. $p > 0.05$, by Student's t test.

DISCUSSION

Here we systematically explored the possibility to use the yeast peroxisomes for production of fatty-acid-derived chemicals. Though peroxisomes play a prominent role in oxidation of toxic or nontoxic "waste" molecules such as fatty acids and H_2O_2, we show that peroxisomes can be harnessed for reductive biosynthesis of fatty-acid-derived chemicals with high value. This "turn waste to value" concept combines several advantages such as a high level of precursor, a more compact space for substrate channelling and an environment without competing pathways.

Peroxisomal targeting of the fatty acyl-CoA reductase FaCoAR enabled a 4-fold higher production of fatty alcohols than the cytosolic pathway (Figure 1). This peroxisomal compartmentalization strategy proved to be even more advantageous for alkane production. In this case, the alkane biosynthesis severely suffered from the strong competition by promiscuous ALR/ADHs[3] present in the cytosol. Side-pathway competition is a consistent challenge in metabolic engineering and often limits the yield of target products. Although blocking competing pathways by deleting corresponding genes is a common strategy, it is challenging to completely delete all ALR/ADHs, because some of them are involved in reductive biosynthesis of essential metabolites.[41] More importantly, many of these ALR/ADHs play an important role in relieving the toxicity of inhibitors present in biomass hydrolysates such as furfural and 5-hydroxymethylfurfural,[42] which is essential for

DOI: 10.1021/jacs.6b07394
J. Am. Chem. Soc. 2016, 138, 15368−15377

future efficient biomass utilization. Peroxisomal compartmentalization improved alkane production by 2-fold and significantly decreased the accumulation of fatty alcohols (Figure 3), which indicated that peroxisomal targeting could reduce the loss of intermediate fatty aldehydes.

Protein fusion and scaffolding strategies have been successfully used for improving cellular substrate channelling.[43−45] However, these strategies sometimes suffer from the loss of enzyme activity and can be challenging for multiprotein pathways due to the difficulty in constructing a functional multidomain enzyme or protein complex. Alternatively, suborganelle compartmentalization of synthetic pathways has been shown to be helpful for biosynthesis. For example, mitochondrial compartmentalization of the respective metabolic pathways improved the production of isoprenoids,[8,9] fusel alcohols[10] and acetoin.[46] These studies showed that organelle compartmentalization can provide a more suitable environment (high level of precursor[10,47] and organelle specific cofactors[8,10]) for biosynthesis of specific products. However, mitochondria are not suitable organelles for alkane production since they contain multiple ADHs[11] that may compete for the fatty aldehydes. We are the first to show that organelle compartmentalization of multiple-step biosynthetic pathways can significantly decrease the accumulation of byproducts by secluding the biosynthetic pathways from efficient competing enzymes (Figure 3). Peroxisomes have been used for production of polyhydroxyalkanoate (PHA)[48−50] and fatty alcohols[51] by expressing a single enzyme to transform the intermediates of fatty acid β-oxidation. Peroxisomes have also been harnessed for production of penicillin in *Aspergillus nidulans* by targeting a cytosolic step of penicillin biosynthesis into peroxisomes for enhanced substrate channeling.[47] We here show that reconstruction of an entire heterologous pathway in the peroxisomes can improve production of a group of chemicals with decreased byproduct accumulation.

As *S. cerevisiae* contains only a very small number of peroxisomes under glucose-rich conditions (Figure S2), it is feasible to increase the peroxisome population for enhanced biosynthesis. Here we show that deletion of *PEX31* and *PEX32* resulted in more and larger peroxisomes and further increased the biosynthesis of fatty acyl-CoA-derived fatty alcohols (Figure 4b and d). However, there was much less of a benefit for alkane production, whereas the byproduct fatty alcohols increased by 50% (Figure 4c). Furthermore, the peroxisomal membrane protein Pex3-GFP was not properly targeted to the peroxisomal membrane (Figure 4d). All these results suggested that the *pex31,32*Δ strain may have an altered peroxisomal membrane structure, which could have resulted in an increased leakage of fatty aldehydes to the cytosol for ALR/ADHs-catalyzed fatty alcohol biosynthesis. As the peroxisome membrane is permeable for metabolites smaller than 400 Da,[13] the fatty aldehydes could partly diffuse across the peroxisome membrane. This is in agreement with the fact that a small amount of fatty alcohol accumulation was observed for the peroxisomal pathways and with the observation that deletion of *HFD1* is still crucial for peroxisomal alkane biosynthesis (Figure 3c). In contrast, *PEX34* overexpression improved alkane production without elevating fatty alcohol accumulation, which might indicate that this constitutively expressed peroxin promoted peroxisome proliferation without increasing membrane permeability. During the preparation of our manuscript, a similar study highlighted the peroxisomal membrane permeability by constructing the peroxisomal prodeoxyviolacein biosynthetic pathway.[52] Our observations here further bring to the attention that engineering peroxisome proliferation may affect the peroxisome (membrane) structure and function, which could affect primary metabolism beyond fatty acid degradation, because peroxisomes play an essential role in those processes, too.[53] Our study therefore also provides new understanding of the biogenesis and metabolism of peroxisomes in yeast.

Finally, peroxisomal targeting of synthetic pathways also improved olefin production (Figure 5), which shows that peroxisomal compartmentalization can be used as a general strategy for production of fatty-acid-derived molecules. Furthermore, this strategy can be used for in vivo evaluation of different enzymes or cofactors (Figure S3), which should be helpful for constructing more efficient pathways for biosynthesis of alkanes and oleo-chemicals.

EXPERIMENTAL PROCEDURES

Yeast Strains, Plasmids, and Reagents. The plasmids and strains used in this study are listed in the Supplementary Tables 1 and 2, respectively. The primers (Supplementary Table 3) were ordered from Sigma-Aldrich. The *SeAAR* and *SeADO* genes were codon-optimized and synthesized as described before.[3] *EcFNR* and *EcFd* were cloned from the genome of *E. coli* DH5α as described before.[3] *FaCoAR*, *MmCAR*, *SeFNR*, *SeFd*, *NpADO*, and *oleT* (Supplementary Table 4) were codon-optimized for yeast expression and synthesized by Genscript. PrimeStar DNA polymerase was purchased from TaKaRa. Zymoprep Yeast Plasmid Miniprep II was supplied by Zymo Research Corp. Restriction enzymes, DNA gel purification and plasmid extraction kits were purchased from ThermoFisher Scientific. Analytical standards for quantification of alkanes, fatty alcohols and terminal alkenes were supplied by Sigma-Aldrich.

Strain Cultivation. Yeast strains were normally cultivated in YPD media consisting of 10 g/L yeast extract (Merck Millipore), 20 g/L peptone (Difco), and 20 g/L glucose (Merck Millipore). Strains containing *URA3* and/or *HIS3* based plasmids/cassettes were selected on synthetic complete media without uracil or L-histidine (SC-URA, SC-HIS or SC-URA-HIS), which consisted of 6.7 g/L yeast nitrogen base (YNB) without amino acids (Formedium), 20 g/L glucose (MerckMillipore), and 0.77 g/L complete supplement mixture without corresponding nutrition (CSM-URA, CSM-HIS or CSM-HIS-URA, Formedium). The *URA3* maker was removed and selected against on SC+5-FOA plates, which contained 6.7 g/L YNB, 0.77 g/L complete supplement mixture, and 0.8 g/L 5-fluoroorotic acid. Strains containing the *amdSYM*[54] cassette were selected on SM media (5 g/L $(NH_4)_2SO_4$, 3 g/L KH_2PO_4, 0.5 g/L $MgSO_4{\cdot}7H_2O$, 6.6 g/L K_2SO_4, 0.6 g/L acetamide, 20 g/L glucose) trace metal and vitamin solutions[55] supplemented with 40 mg/L histidine, and/or 60 mg/L uracil if needed). Strains containing the *kanMX* cassette were selected on YPD plates containing 200 mg/L G418 (Formedium).

Shake flask batch fermentations for production of alkanes, fatty alcohols and olefins were carried out in minimal medium containing 5 g/L $(NH_4)_2SO_4$, 3 g/L KH_2PO_4, 0.5 g/L $MgSO_4{\cdot}7H_2O$, 30 g/L glucose, trace metal and vitamin solutions[55] supplemented with 40 mg/L histidine, and/or 60 mg/L uracil if needed. Cultures were inoculated, from 24 h precultures, at an initial OD_{600} of 0.1 in 15 mL minimal medium and cultivated at 200 rpm, 30 °C for 72 h.

Genetic Engineering. All episomal vectors or genome-integrated pathways (Figure S9) were constructed by the modular pathway engineering (MOPE) strategy.[44] Briefly, genes, promoters, and terminators were amplified from the yeast genome or the custom synthesized templates. Then, gene expression modules, consisting of a promoter, a structural gene, a terminator, and the promoter of the next module for homologous recombination, were assembled by one-pot fusion PCR.[44] The modules were gel purified and transformed to the *S. cerevisiae*. Scarless gene deletion was performed[56] by using a *Kluyveromyces lactis URA3* (*KlURA3*) gene as selection marker. The deletion cassettes were constructed by fusing 200−600 nucleotide homologous arms with *KlURA3*. The respective *S. cerevisiae* strains

DOI: 10.1021/jacs.6b07394
J. Am. Chem. Soc. 2016, 138, 15368−15377

were transformed with the deletion cassettes and selected on SC-URA plates. Positive clones were plated on SC+FOA plates for looping out the *KIURA3* marker via the direct repeats. An *amdSYM* cassette[54] with 80-bp homologous arms was used for *PEX31* deletion.

During construction of YJZ74, it was difficult to delete *PEX32* based on the *pex31Δ::amdSYM* in strain YJZ63 for unknown reasons. Considering the use of the same promoter and terminator in *amdSYM* cassette, the available *kanMX* cassettes was not suitable for subsequent *PEX32* deletion in strain YJZ63 harboring *pex31Δ::amdSYM*. We first tried a *URA3* cassette with 80-bp homologous arms, however, the loop-out of the *URA3* cassette failed three times. Then we constructed three alternative *kanMX* cassettes: *kanMX*-PX1 with promoter *TEF1p* and terminator *PEX32t*, *kanMX*-PX2 only containing the *kanMX* open reading frame without promoter and terminator, and *kanMX*-PX3 with promoter *tHXT7p* and terminator *PEX32t*. Interestingly, replacing *PEX32* in YJZ63 was successful with the *kanMX*-PX3 cassette, which indicated the expression level of *kanMX* should be carefully tuned for deletion of some specific genes. The genomic manipulations were verified with colony PCR by using the genomic DNA, which was prepared by a quick extraction method as previously described.[57]

Product Extraction and Quantification. Extraction and quantification of fatty alcohols, alkanes and olefins were performed as described in a previous report[3] with slight modifications. Briefly, fatty alcohols were analyzed by gas chromatography (Focus GC, ThermoFisher Scientific) equipped with a Zebron ZB-5MS GUARDIAN capillary column (30 m × 0.25 mm × 0.25 μm, Phenomenex) and a flame ionization detector (FID, ThermoFisher Scientific). The GC program for fatty alcohol quantification was as follows: initial temperature of 45 °C hold for 2.5 min; then ramp to 220 °C at a rate of 20 °C per min and hold for 2 min; ramp to 300 °C at a rate of 20 °C per min and hold for 5 min. The temperature of the inlet and detector were kept at 280 and 300 °C, respectively.

Alkanes and olefins were analyzed by a GC-MS (Focus GC with a DSQII mass spectrometer ThermoFisher Scientific) equipped with a Zebron ZB-5MS GUARDIAN capillary column (30 m × 0.25 mm × 0.25 μm, Phenomenex). The GC program for alkanes was as follows: initial temperature of 50 °C, hold for 5 min; then ramp to 140 °C at a rate of 10 °C per min and hold for 10 min; ramp to 310 °C at a rate of 15 °C per min and hold for 7 min. The olefin GC program was: initial temperature of 50 °C, hold for 5 min; then ramp to 310 °C at a rate of 10 °C per min and hold for 6 min. The temperature of inlet, mass transfer line and ion source were kept at 250, 300, and 230 °C, respectively. The flow rate of the carrier gas (helium) was set to 1.0 mL per minute, and data were acquired at full scan mode (50−650 *m*/*z*) and then analyzed by using the Xcalibur software. Since there was no available standards for 7-pentadecene, it was identified by comparing extract product from the alkane producing strain and the control strain (Figure S10) and search in the NIST library. 7-Pentadecene and 7-heptadecene were quantified by using the standard curves of pentadecane and heptadecane, respectively. This quantification strategy based on the response coefficients (peak area/concentration) are almost identical for C14−C20 alkanes, 1-pentadecene, and 1-heptadecene.

Enzymatic Assay. Cells (8 mL) that had been cultivated for 48 h were harvested by centrifugation (4000*g*, 5 min, 4 °C) and washed with cold buffer[58] (10 mM potassium phosphate, 2 mM EDTA, pH 7.5). Cell pellets were resuspended in 0.5 mL of extraction buffer (50 mM potassium phosphate, 1 mM EDTA, 1 mM KCl, pH 7.5) containing 10 mM DTT (Sigma), 1% (V/V) protease inhibitor (ThermoFisher Scientific) and 15 U 100T Zymolyase (Zymo Research). The cell suspensions were incubated at 37 °C for 60 min and then vortexed for 30 s with 300 mg 0.2−0.4 mm glass beads. After disruption, samples were centrifuged at 20 000*g* at 0 °C for 20 min, and the supernatants were used as cell-free extracts for enzymatic assay. The protein concentrations were quantified by using a DC Protein Assay kit (Bio-Rad) according to the instruction manual.

The MmCAR activity assay was performed in 96-well microplates with 100 μL of reaction mixture (50 mM Tris-Cl, 10 mM $MgCl_2$ pH 7.5, 1 mM NADPH, 1 mM ATP and 0.5 mM palmitoleic acid). Then 10 μL of cell-free extract (about 5 μg total protein) was added to initiate the reaction. The reaction was monitored at 340 nm for 20 min with a FLUOstar Omega microplate reader (BMG LABTECH GmbH). One unit (U) MmCAR activity was defined as NADPH oxidation rate of 1 μM/min.

Fluorescence Microscopy Analysis. For confirmation of the protein localization, the C-termini of the proteins were fused to a green fluorescent protein (GFP) carrying peroxisomal signal with a flexible linker GGGS, and then the encoding genes were transformed into the yeast strain EY1673 expressing a peroxisome marker protein Pex3 with a C-terminal RFP tag.[12] The cells were cultivated in SC-URA or minimal media for 48 h at 30 °C, 200 rpm. Three μL of the cell cultures were dropped onto microscope slides and then viewed with a LEICA DM2000 microscope (Leica Microsystems CMS GmbH). For verification of the peroxisomal targeting of the whole alkane biosynthesis pathway, the plasmid pFluores6 (for expression of SeAAR fused with RFP and SeADO fused with GFP) was transformed into YJZ03 and YJZ62. The cells were cultivated in minimal media for 36 h and 3 μL cell cultures were dropped onto microscope slides and then viewed with a LEICA DM2000 microscope.

■ ASSOCIATED CONTENT

Supporting Information

The Supporting Information is available free of charge on the ACS Publications website at DOI: 10.1021/jacs.6b07394.

Figure S1: Optimizing the context of the peroxisomal targeting signal. Figure S2: confirmation of peroxisomal targeting. Figure S3: Alkane production by strains carrying different pathways. Figure S4: Peroxisomal or cytosolic fatty alcohol production in S288c background strain carrying different combinations of PEX30, 31 and/or 32 deletion. Figure S5: Engineering peroxisome biogenesis for alkane production. Figure S6: Specific alkane titers of the yeast cells with cytosolic and peroxisomal alkane pathways. Figure S7: Engineering peroxins improved alkane production from peroxisomal pathways but not the cytosolic ones. Figure S8: Comparing the cytosolic and peroxisomal pathways for olefin production. Figure S9: Genetic arrangement of pathways on episomal plasmids or integrated into a chromosome. Figure S10: Representative gas chromatograms (GC) of yeast extracts of corresponding strains. Supplementary Table 1: Plasmids used in this study. Supplementary Table 2: *S. cerevisiae* strains. Supplementary Table 3: Primers used in this study. Supplementary Table 4: Codon optimized genes. (PDF)

■ AUTHOR INFORMATION

Corresponding Authors

*yongjin@chalmers.se or zhouyongjin100@gmail.com
*nielsenj@chalmers.se

Present Address

⊥N.A.B.: Evolva Biotech, Lersø Parkallé 40-42, DK-2100, Copenhagen, Denmark.

Author Contributions

#Y.J.Z. and N.A.B. contributed equally.

Notes

The authors declare the following competing financial interest(s): Y.J.Z, N.A.B., V.S., and J.N. have filed a patent (Engineering of hydrocarbon metabolism in yeast, No. WO2015057155 A1) for protection of part of this work. All other authors declare no competing financial interests.

DOI: 10.1021/jacs.6b07394
J. Am. Chem. Soc. 2016, 138, 15368−15377

■ ACKNOWLEDGMENTS

This work was funded by the Knut and Alice Wallenberg Foundation, the Novo Nordisk Foundation, Vetenskapsrådet and FORMAS. This work is part of a collaborative project between Chalmers and Total. We thank Prof. Richard A. Rachubinski (University of Alberta, Canada) for kindly providing the *pex30-32Δ* strains with an S288c background, and Prof. Erin K. O'Shea (Harvard University, USA) for providing the RFP-tagged Pex3 strain EY1673. We thank Dr. Mingtao Huang for helping with the enzymatic assay and fluorescence microscopy analysis. We also thank Sakda Khoomrung and the Chalmers Mass Spectrometry Infrastructure (Jacob Kindbom, Julia Karlsson and Otto Savolainen) for assistance with GC-MS analysis. We also appreciate the helpful discussions with Zongjie Dai, Mingtao Huang, Jiufu Qin, Paulo Teixeira, Paul Hudson (KTH, Stockholm, Sweden), and Rahul Kumar.

■ REFERENCES

(1) Dydio, P.; Detz, R. J.; de Bruin, B.; Reek, J. N. *J. Am. Chem. Soc.* **2014**, *136*, 8418.
(2) Kunjapur, A. M.; Tarasova, Y.; Prather, K. L. *J. Am. Chem. Soc.* **2014**, *136*, 11644.
(3) Buijs, N. A.; Zhou, Y. J.; Siewers, V.; Nielsen, J. *Biotechnol. Bioeng.* **2015**, *112*, 1275.
(4) Zhou, Y. J.; Buijs, N. A.; Zhu, Z.; Qin, J.; Siewers, V.; Nielsen, J. *Nat. Commun.* **2016**, *7*, 11709.
(5) Kaluzna, I. A.; Matsuda, T.; Sewell, A. K.; Stewart, J. D. *J. Am. Chem. Soc.* **2004**, *126*, 12827.
(6) Andre, C.; Kim, S. W.; Yu, X. H.; Shanklin, J. *Proc. Natl. Acad. Sci. U. S. A.* **2013**, *110*, 3191.
(7) Zhou, Y. J.; Buijs, N. A.; Siewers, V.; Nielsen, J. *Front. Bioeng. Biotechnol.* **2014**, *2*, 32.
(8) Szczebara, F. M.; Chandelier, C.; Villeret, C.; Masurel, A.; Bourot, S.; Duport, C.; Blanchard, S.; Groisillier, A.; Testet, E.; Costaglioli, P.; Cauet, G.; Degryse, E.; Balbuena, D.; Winter, J.; Achstetter, T.; Spagnoli, R.; Pompon, D.; Dumas, B. *Nat. Biotechnol.* **2003**, *21*, 143.
(9) Farhi, M.; Marhevka, E.; Masci, T.; Marcos, E.; Eyal, Y.; Ovadis, M.; Abeliovich, H.; Vainstein, A. *Metab. Eng.* **2011**, *13*, 474.
(10) Avalos, J. L.; Fink, G. R.; Stephanopoulos, G. *Nat. Biotechnol.* **2013**, *31*, 335.
(11) Wiesenfeld, M.; Schimpfessel, L.; Crokaert, R. *Biochim. Biophys. Acta, Protein Struct.* **1975**, *405*, 500.
(12) Huh, W. K.; Falvo, J. V.; Gerke, L. C.; Carroll, A. S.; Howson, R. W.; Weissman, J. S.; O'Shea, E. K. *Nature* **2003**, *425*, 686.
(13) Stehlik, T.; Sandrock, B.; Ast, J.; Freitag, J. *Curr. Opin. Microbiol.* **2014**, *22*, 8.
(14) Henke, B.; Girzalsky, W.; Berteaux-Lecellier, V.; Erdmann, R. *J. Biol. Chem.* **1998**, *273*, 3702.
(15) Hiltunen, J. K.; Mursula, A. M.; Rottensteiner, H.; Wierenga, R. K.; Kastaniotis, A. J.; Gurvitz, A. *FEMS Microbiol. Rev.* **2003**, *27*, 35.
(16) van Roermund, C. W.; Hettema, E. H.; Kal, A. J.; van den Berg, M.; Tabak, H. F.; Wanders, R. J. *EMBO J.* **1998**, *17*, 677.
(17) Rottensteiner, H.; Theodoulou, F. L. *Biochim. Biophys. Acta, Mol. Cell Res.* **2006**, *1763*, 1527.
(18) Willis, R. M.; Wahlen, B. D.; Seefeldt, L. C.; Barney, B. M. *Biochemistry* **2011**, *50*, 10550.
(19) Valle-Rodriguez, J. O.; Shi, S. B.; Siewers, V.; Nielsen, J. *Appl. Energy* **2014**, *115*, 226.
(20) Feng, X.; Lian, J.; Zhao, H. *Metab. Eng.* **2015**, *27*, 10.
(21) Lennen, R. M.; Pfleger, B. F. *Curr. Opin. Biotechnol.* **2013**, *24*, 1044.
(22) Foo, J. L.; Susanto, A. V.; Keasling, J. D.; Leong, S. S.; Chang, M. W. *Biotechnol. Bioeng.* **2016**, DOI: 10.1002/bit.25920.
(23) Rodriguez, G. M.; Atsumi, S. *Metab. Eng.* **2014**, *25*, 227.
(24) Hazelwood, L. A.; Daran, J. M.; van Maris, A. J.; Pronk, J. T.; Dickinson, J. R. *Appl. Environ. Microb.* **2008**, *74*, 2259.
(25) Agapakis, C. M.; Boyle, P. M.; Silver, P. A. *Nat. Chem. Biol.* **2012**, *8*, 527.
(26) Schirmer, A.; Rude, M. A.; Li, X.; Popova, E.; del Cardayre, S. B. *Science* **2010**, *329*, 559.
(27) Zhang, J. J.; Lu, X. F.; Li, J. J. *Biotechnol. Biofuels* **2013**, *6*, 86.
(28) Wang, Q.; Huang, X.; Zhang, J.; Lu, X.; Li, S.; Li, J. J. *Chem. Commun.* **2014**, *50*, 4299.
(29) Akhtar, M. K.; Turner, N. J.; Jones, P. R. *Proc. Natl. Acad. Sci. U. S. A.* **2013**, *110*, 87.
(30) Saraya, R.; Veenhuis, M.; van der Klei, I. J. *FEBS J.* **2010**, *277*, 3279.
(31) Vizeacoumar, F. J.; Torres-Guzman, J. C.; Bouard, D.; Aitchison, J. D.; Rachubinski, R. A. *Mol. Biol. Cell* **2004**, *15*, 665.
(32) Tower, R. J.; Fagarasanu, A.; Aitchison, J. D.; Rachubinski, R. A. *Mol. Biol. Cell* **2011**, *22*, 1727.
(33) Tam, Y. Y.; Torres-Guzman, J. C.; Vizeacoumar, F. J.; Smith, J. J.; Marelli, M.; Aitchison, J. D.; Rachubinski, R. A. *Mol. Biol. Cell* **2003**, *14*, 4089.
(34) Mindthoff, S.; Grunau, S.; Steinfort, L. L.; Girzalsky, W.; Hiltunen, J. K.; Erdmann, R.; Antonenkov, V. D. *Biochim. Biophys. Acta, Mol. Cell Res.* **2016**, *1863*, 271.
(35) Liu, Q.; Wu, K.; Cheng, Y.; Lu, L.; Xiao, E.; Zhang, Y.; Deng, Z.; Liu, T. *Metab. Eng.* **2015**, *28*, 82.
(36) Mendez-Perez, D.; Begemann, M. B.; Pfleger, B. F. *Appl. Environ. Microb.* **2011**, *77*, 4264.
(37) Rude, M. A.; Baron, T. S.; Brubaker, S.; Alibhai, M.; Del Cardayre, S. B.; Schirmer, A. *Appl. Environ. Microb.* **2011**, *77*, 1718.
(38) Rui, Z.; Li, X.; Zhu, X.; Liu, J.; Domigan, B.; Barr, I.; Cate, J. H.; Zhang, W. *Proc. Natl. Acad. Sci. U. S. A.* **2014**, *111*, 18237.
(39) Chen, B.; Lee, D. Y.; Chang, M. W. *Metab. Eng.* **2015**, *31*, 53.
(40) Liu, Y.; Wang, C.; Yan, J.; Zhang, W.; Guan, W.; Lu, X.; Li, S. *Biotechnol. Biofuels* **2014**, *7*, 28.
(41) Ehmann, D. E.; Gehring, A. M.; Walsh, C. T. *Biochemistry* **1999**, *38*, 6171.
(42) Jordan, D. B.; Braker, J. D.; Bowman, M. J.; Vermillion, K. E.; Moon, J.; Liu, Z. L. *Biochim. Biophys. Acta, Proteins Proteomics* **2011**, *1814*, 1686.
(43) Dueber, J. E.; Wu, G. C.; Malmirchegini, G. R.; Moon, T. S.; Petzold, C. J.; Ullal, A. V.; Prather, K. L. J.; Keasling, J. D. *Nat. Biotechnol.* **2009**, *27*, 753.
(44) Zhou, Y. J.; Gao, W.; Rong, Q.; Jin, G.; Chu, H.; Liu, W.; Yang, W.; Zhu, Z.; Li, G.; Zhu, G.; Huang, L.; Zhao, Z. K. *J. Am. Chem. Soc.* **2012**, *134*, 3234.
(45) Conrado, R. J.; Wu, G. C.; Boock, J. T.; Xu, H.; Chen, S. Y.; Lebar, T.; Turnsek, J.; Tomsic, N.; Avbelj, M.; Gaber, R.; Koprivnjak, T.; Mori, J.; Glavnik, V.; Vovk, I.; Bencina, M.; Hodnik, V.; Anderluh, G.; Dueber, J. E.; Jerala, R.; DeLisa, M. P. *Nucleic Acids Res.* **2012**, *40*, 1879.
(46) Li, S.; Liu, L.; Chen, J. *Metab. Eng.* **2015**, *28*, 1.
(47) Herr, A.; Fischer, R. *Metab. Eng.* **2014**, *25*, 131.
(48) De Oliveira, V. C.; Maeda, I.; Delessert, S.; Poirier, Y. *Appl. Environ. Microb* **2004**, *70*, 5685.
(49) Poirier, Y.; Erard, N.; Petétot, J. M. *FEMS Microbiol. Lett.* **2002**, *207*, 97.
(50) Poirier, Y.; Erard, N.; Petétot, J. M. *Appl. Environ. Microb* **2001**, *67*, 5254.
(51) Sheng, J.; Stevens, J.; Feng, X. *Sci. Rep.* **2016**, *6*, 26884.
(52) DeLoache, W. C.; Russ, Z. N.; Dueber, J. E. *Nat. Commun.* **2016**, *7*, 11152.
(53) Freitag, J.; Ast, J.; Bolker, M. *Nature* **2012**, *485*, 522.
(54) Solis-Escalante, D.; Kuijpers, N. G.; Bongaerts, N.; Bolat, I.; Bosman, L.; Pronk, J. T.; Daran, J. M.; Daran-Lapujade, P. *FEMS Yeast Res.* **2013**, *13*, 126.
(55) Verduyn, C.; Postma, E.; Scheffers, W. A.; Van Dijken, J. P. *Yeast* **1992**, *8*, 501.
(56) Akada, R.; Kitagawa, T.; Kaneko, S.; Toyonaga, D.; Ito, S.; Kakihara, Y.; Hoshida, H.; Morimura, S.; Kondo, A.; Kida, K. *Yeast* **2006**, *23*, 399.

DOI: 10.1021/jacs.6b07394
J. Am. Chem. Soc. 2016, 138, 15368−15377

(57) Looke, M.; Kristjuhan, K.; Kristjuhan, A. *Biotechniques* **2011**, *50*, 325.
(58) Moller, K.; Bro, C.; Pikur, J.; Nielsen, J.; Olsson, L. *FEMS Yeast Res.* **2002**, *2*, 233.

DOI: 10.1021/jacs.6b07394
J. Am. Chem. Soc. 2016, 138, 15368−15377